ACS Catalysis

LETTER

pubs.acs.org/acscatalysis

Synthesis of Pt_3Sn Alloy Nanoparticles and Their Catalysis for Electro-Oxidation of CO and Methanol

Yi Liu,[†] Dongguo Li,[†,‡] Vojislav R. Stamenkovic,[‡] Stuart Soled,[§] Juan D. Henao,[§] and Shouheng Sun*[,†]

[†]Department of Chemistry, Brown University, Providence, Rhode Island 02912, United States

[‡]Materials Science Division, Argonne National Laboratory, Argonne, Illinois 60439, United States

[§]ExxonMobil Research and Engineering Co., Annandale, New Jersey 08801, United States

Supporting Information

ABSTRACT: Monodisperse Pt_3Sn alloy nanoparticles (NPs) were synthesized by a controlled coreduction of Pt(II) acetylacetonate and Sn(II) acetylacetonate at 180−280 °C in 1-octadecene. In the synthesis, oleylamine was used as a reducing agent, and oleylamine/oleic acid served as surfactants. The sizes of the Pt_3Sn NPs were tuned from 4 to 7 nm by controlling the metal salt injection temperatures from 180 to 240 °C. These monodisperse Pt_3Sn NPs were highly active for CO and methanol oxidation in 0.1 M $HClO_4$ solutions, and their activity and stability could be further improved by a postsynthesis thermal treatment at 400 °C in Ar + 5% H_2 for 1 h. They are promising as a practical catalyst for CO and methanol oxidation reactions in polymer electrolyte membrane fuel cell conditions.

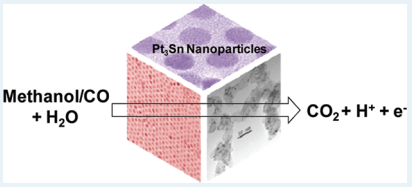

KEYWORDS: Pt_3Sn nanoparticles, synthesis, CO oxidation, methanol oxidation, catalysis

Alloying a non-noble metal (M) with Pt has become a popular approach to Pt-based catalysts with much reduced Pt usage and enhanced Pt activity.[1−7] Depending on the chemical nature of M, PtM can be made highly active for either electrochemical oxidation or reduction.[5−8] Among various PtM alloys studied thus far, PtSn alloys represent an interesting group of catalysts not only for hydrogenation[9−11] and dehydrogenation reactions,[12−14] but also for electro-oxidation of carbon monoxide (CO),[15−20] methanol,[21−23] ethanol,[23−26] and ethylene glycol.[27] Previous evaluations on single crystals and thin films of Pt_3Sn for catalytic CO oxidation suggest that Sn as an alloy component can enhance CO oxidation on Pt by promoting H_2O dissociation on Sn to form Sn−OH and by altering electronic properties of Pt through its bonding with Pt, weakening the CO adsorption on Pt.[15−19] These experimental observations are further supported by the first-principles and density function theory calculations.[8,28] The activation energies for CO oxidation on Pt_3Sn/Pt (111), Pt_3Sn (111), and Pt (111) surfaces are 0.64 eV, 0.68, and 0.82 eV, respectively,[28] and water dissociation energy is lower on Sn (0.44 eV) than on Pt (0.67 eV).[8] These studies indicate that PtSn alloys in a nanoparticle (NP) form should be a more promising catalyst for CO and other small organic molecule oxidizations.

In this paper, we report a high temperature organic phase synthesis of monodisperse Pt_3Sn alloy NPs by coreduction of Pt and Sn salts and study their enhanced catalysis for CO and methanol oxidation reaction (MOR) in acid solutions. Previously, Pt_3Sn NPs were synthesized directly on carbon supports from reduction of the absorbed Pt salt and Sn salt.[20] Recently, Pt_3Sn NPs were prepared by room temperature H_2 reduction of Pt(dibenzylidene acetone)$_2$ with $(n\text{-Bu})_3SnH$,[29] or made by high temperature coreduction of Pt(acac)$_2$ (acac = acetylacetonate) and Sn(acac)$_2$ with 1,2-hexandecanediol.[21] These Pt_3Sn NPs were examined for CO oxidation and MOR catalysis and were found to be unstable in acidic electrolyte and oxidative conditions.[21] By carefully optimizing the synthesis conditions, we succeeded in synthesizing monodisperse Pt_3Sn NPs with controlled sizes, composition, and alloy structure. These Pt_3Sn NPs were highly active for CO and methanol oxidation in 0.1 M $HClO_4$ solutions, and their activity and stability were further improved by a postsynthesis thermal treatment. These Pt_3Sn NPs could serve as a promising new CO tolerant catalyst for oxidation of small organic molecules.

Monodisperse Pt_3Sn alloy NPs were synthesized by high temperature reduction of Pt(acac)$_2$ and Sn(acac)$_2$. In the synthesis, oleylamine (OAm), as well as the solution of Pt(acac)$_2$ and Sn(acac)$_2$ in benzyl ether (BE) was injected into the solution of oleic acid (OA) in 1-octadecene (ODE) at 220 °C. The reaction temperature was subsequently raised to 280 °C and kept at this temperature for 1 h to complete the reduction. Transmission electron microscopy (TEM) analysis shows that the as-synthesized Pt_3Sn alloy NPs are monodisperse with their diameter measured to be 5.2 ± 0.4 nm (Figure 1A). Selected area diffraction (SAED) pattern of a group of NPs (Figure 1B) and high resolution TEM (HRTEM) of a representative single NP (Figure 1C) indicate that the NPs are highly crystallized. The crystalline fringe shown in Figure 1C is measured to be ~0.23 nm, corresponding to the (111) interplanar spacing of the face centered cubic (fcc) Pt_3Sn alloy structure (0.231 nm). Figure 1D is the X-ray diffraction (XRD) pattern of the as-synthesized Pt_3Sn NPs. The XRD peaks match with the fcc Pt_3Sn

Received: August 20, 2011
Revised: November 3, 2011
Published: November 04, 2011

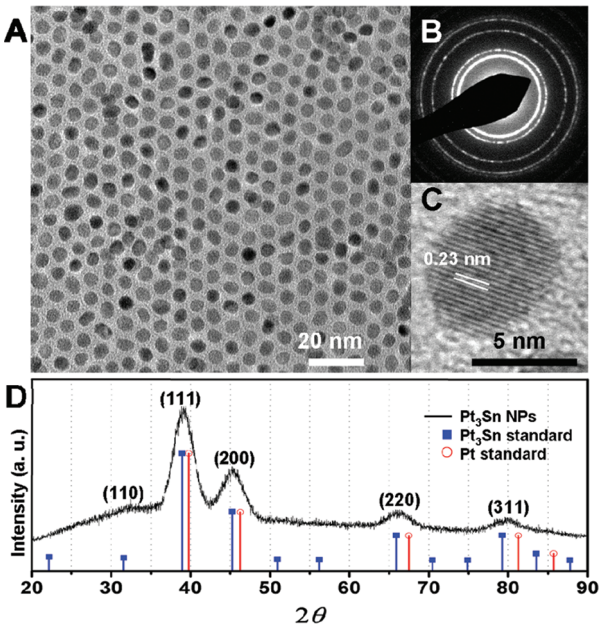

Figure 1. (A) TEM image, (B) SAED pattern, (C) HRTEM image, (D) XRD pattern of the as-synthesized 5.2 ± 0.4 nm Pt_3Sn NPs. The drop lines are the standard peaks for Pt_3Sn (blue solid squares, PDF 03-065-0958) and Pt (red open circles, PDF 01-084-0646).

standard, and shift to lower diffraction angles compared to the fcc Pt peaks, indicating that alloying Pt with Sn results in a crystal lattice expansion in Pt_3Sn NPs. The composition of the Pt_3Sn NPs was measured to be 71/29 (atomic ratio) by both inductively coupled plasma-atomic emission spectrometry (ICP-AES) and Energy Dispersive X-ray Spectroscopy (EDS) (Supporting Information, Figure S1).

In the synthesis, the size of the Pt_3Sn NPs was tuned by controlling the precursor injection temperatures. Injection at 180 °C resulted in 3.6 ± 0.3 nm NPs while at 240 °C led to 6.6 ± 0.9 nm NPs (Supporting Information, Figure S2). We should emphasize that injection of $Pt(acac)_2$ and $Sn(acac)_2$ at higher temperatures and the use of OAm as the reducing agent are essential for the successful synthesis of monodisperse Pt_3Sn alloy NPs. Since $Sn(acac)_2$ is moisture sensitive, injecting $Sn(acac)_2$ and $Pt(acac)_2$ together at high temperatures can inhibit the hydrolysis of $Sn(acac)_2$ and promote the alloy formation. If $Sn(acac)_2$ was added before the reaction solution was heated, the side reaction of hydrolysis would lead to much less control in NP composition and morphology (Supporting Information, Figure S3A). OAm served as a mild reducing agent for coreduction of Pt and Sn salts at high temperatures. A stronger reducing agent, such as morphine borane, tended to reduce Pt selectively, producing nonuniform Pt-rich PtSn (Supporting Information, Figure S3B,D). In a control experiment, we found that the presence of $Pt(acac)_2$ and $Sn(acac)_2$ in the injection solution could actually facilitate the reduction of these two salts for the formation of PtSn alloy. Without $Pt(acac)_2$, $Sn(acac)_2$ could not be reduced completely to its metallic state. Instead, a mixture of Sn and SnO NPs was separated (Supporting Information, Figures S3C,E). On the other hand, $Sn(acac)_2$ also helped Pt nucleation and growth. Without $Sn(acac)_2$, the reaction at the same condition could only lead to the formation of subnanometer Pt NPs which were difficult to precipitate from the reaction

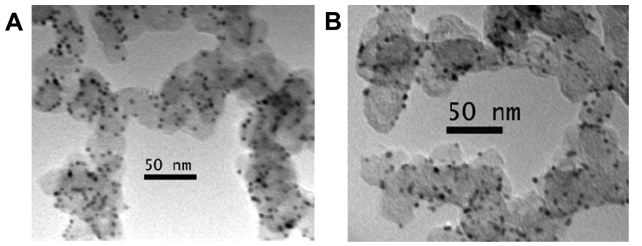

Figure 2. TEM images of (A) the Pt_3Sn as prepared and (B) the Pt_3Sn annealed. The catalysts were deposited on carbon black (Ketjen EC-300J) and washed with acetic acid (A) and annealed under Ar + 5% H_2 at 400 °C for 1 h (B).

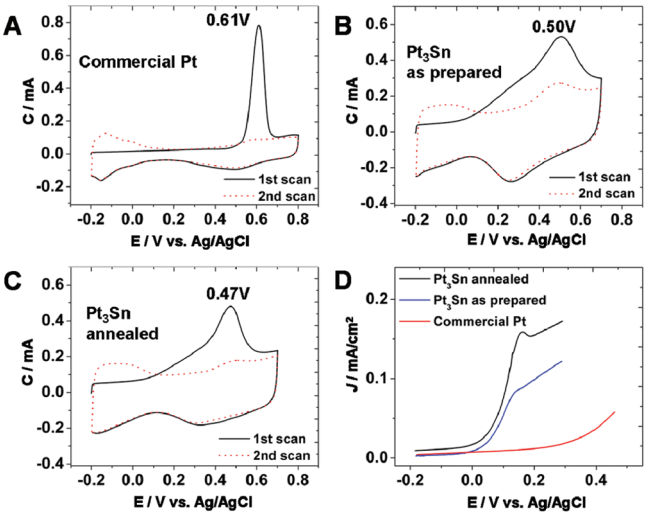

Figure 3. CO strippings of (A) the commercial Pt, (B) the Pt_3Sn as prepared, (C) the Pt_3Sn annealed. (D) J-V curves reflecting CO oxidation catalyzed by different catalysts in CO saturated 0.1 M $HClO_4$. The curves were obtained at a potential sweeping rate of 20 mV/s and RDE rotation speed of 1600 rpm.

solution. Our synthesis indicates that the coexistence of $Sn(acac)_2$ and $Pt(acac)_2$ is important for the metal salt coreduction, metal conucleation, and growth into Pt_3Sn NPs.

The Pt_3Sn NPs were deposited on carbon black (Ketjen EC-300J) for catalytic studies as described in the experimental section. Figure 2 shows the TEM images of two kinds of Pt_3Sn catalysts studied in this work. By comparing the Pt_3Sn as prepared (Figure 2A), and Pt_3Sn annealed (Figure 2B), we can see that the NPs have no obvious change in particle size during the acetic acid and the thermal treatment. XRDs of the Pt_3Sn as prepared and Pt_3Sn annealed (Supporting Information, Figure S4) suggest a slight crystalline size increase from 3 to 3.6 nm. This crystalline size increase is due to the crystalline domain growth within a single NP, not the NP aggregation/sintering.

CO electro-oxidation serves as a model system in understanding electro-oxidation of methanol.[30,31] CO stripping voltammograms were used to probe oxidation potentials of the adsorbed CO on catalyst surface. Figure 3A−C summarizes the results on CO stripping experiments. The commercial Pt has a sharp oxidation peak at 0.61 V, and the as-prepared and as-annealed Pt_3Sn show broader peaks at 0.50 and 0.47 V. These broader oxidation peaks infer the lower onset potential

dx.doi.org/10.1021/cs200430r |ACS Catal. 2011, 1, 1719–1723

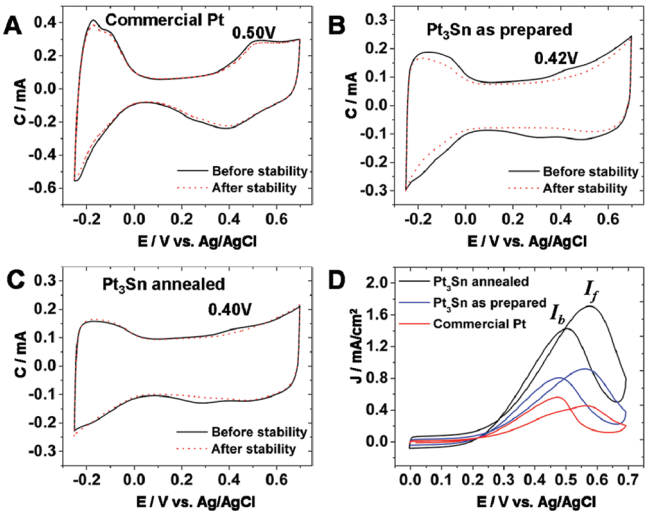

Figure 4. CVs of (A) the commercial Pt, (B) the Pt_3Sn as prepared, and (C) the Pt_3Sn annealed. (D) J-V curves reflecting MOR catalysis in 0.1 M $HClO_4$ and 0.1 M methanol with a potential sweeping rate at 50 mV/s.

for electro-oxidation of "weakly adsorbed" CO.[19−21] Figure 3D shows the CO oxidation curves in which the onset potentials are ~0 V for both Pt_3Sn NP catalysts and 0.25 V for the Pt catalyst. The annealed Pt_3Sn/C has the slightly higher activity than the as prepared one as indicated by the slightly negative shift of the CO stripping peak and higher CO oxidation current density. The enhanced CO oxidation activity of the Pt_3Sn alloy NPs over Pt NPs is consistent with what has been reported in the single crystal and thin film studies.[15−19] In the PtSn alloy structure, Sn weakens the CO adsorption on Pt and promotes water dissociation to form $Sn-OH_{ad}$ near Pt-CO, facilitating the fast CO oxidation.[15]

The cyclic voltammograms (CVs) (Figure 4A−C) were recorded in 0.1 M $HClO_4$. The hydrogen under potential desorption area (H_{upd}) was used to estimate the electrochemically active surface areas (ECASAs) of the catalysts. The ECASA is comparably small for the as-prepared Pt_3Sn (1.99 cm^2). This is further reduced to 1.14 cm^2 for the annealed Pt_3Sn due likely to the increase of Sn on the alloy NP surface and the nonadsorption of H_{upd} on Sn.

The CO stripping experiments indicate that monodisperse Pt_3Sn alloy NPs are active for CO oxidation and should be a good catalyst for MOR. The MOR activity was measured by sweeping the potentials from 0−0.7 V in a solution of 0.1 M $HClO_4$ and 0.1 M methanol, and the current density was normalized by dividing the raw current with the ECASAs, as shown in Figure 4D. We can see that the annealed Pt_3Sn has the highest oxidation peak current density in the forward scan (I_f). The I_f (mA/cm^2) decreases from the as-annealed Pt_3Sn (1.71) to the as-prepared Pt_3Sn (0.92) and further to the commercial Pt (0.45). The CO tolerance of the catalyst can be evaluated by the ratio of the oxidation peak current densities in the forward and backward scans (I_f/I_b). Larger I_f/I_b represents a more complete MOR, less accumulation of CO_{ads}, and a better CO-poisoning tolerance.[32] I_f/I_b ratios are calculated from the MORs in Figure 4D to be 1.20, 1.14, and 0.80 for the annealed Pt_3Sn, as-prepared Pt_3Sn, and commercial Pt, respectively. The MOR currents normalized to Pt weight are given in Supporting Information, Figure S5. The mass

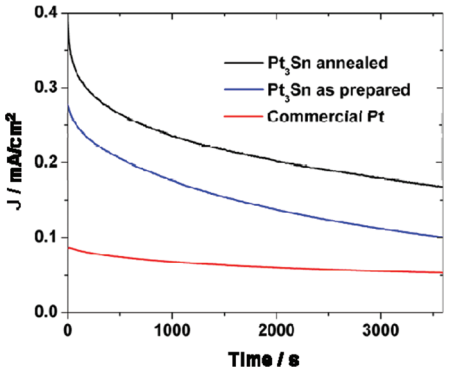

Figure 5. Chronoamperometric curves reflecting stability of the NP catalysts in 0.1 M $HClO_4$ and 0.1 M methanol at constant voltage 0.3 V for 1 h.

current densities follow the order of Pt_3Sn annealed > Pt > Pt_3Sn as prepared. The lower mass activity of the as-prepared Pt_3Sn is likely caused by their larger size (5.2 nm) and less perfect alloy structure. Once annealed, these Pt_3Sn NPs form a better alloy structure and may show more synergetic effect from Pt−Sn for MOR, leading to higher activity.

Stability of the catalyst in the oxidation conditions has long been a concern in developing Pt alloy catalysts for practical applications. The stability of the Pt_3Sn NP catalysts were evaluated by the chronoamperometric curves in 0.1 M $HClO_4$ + 0.1 M methanol at 0.3 V for 1 h (Figure 5). The Pt_3Sn annealed shows less degradation in current density compared to the Pt_3Sn as-prepared, and both kinds of Pt_3Sn NPs have higher current density than the commercial Pt throughout the 1 h test period. The CVs of the catalysts in 0.1 M $HClO_4$ before and after the 1 h stability test are compared in Figure 4A−C. The commercial Pt has an ECASA decrease from 5.15 cm^2 to 4.55 cm^2 (−11.7%), which agrees with the NP aggregation observed after catalysis (Supporting Information, Figure S6A,B). The as-prepared Pt_3Sn NPs are unstable and show certain degree of aggregation (Supporting Information, Figure S6C) with ECASA changing from 1.99 cm^2 to 1.54 cm^2 (−22.6%). Their composition is changed from Pt/Sn = 70/30 to 77/23 (Supporting Information, Figure S1). In contrast, the annealed Pt_3Sn NPs show a much improved stability without obvious change in both NP morphology (Supporting Information, Figure S6D) and composition (from Pt/Sn = 70/30 to 72/28, Supporting Information, Figure S1). Their ECASA area is actually increased from 1.14 to 1.27 cm^2 (+11.4%) due most likely to the more efficient H_2 adsorption/desorption on the better ordered PtSn alloy structure.

In summary, we have developed a high temperature organic phase synthesis of monodisperse Pt_3Sn alloy NPs by a controlled coreduction of $Pt(acac)_2$ and $Sn(acac)_2$ at 180−280 °C in 1-octadecene. In the synthesis, oleylamine was used as a reducing agent and oleylamine/oleic acid served as surfactants. The key to the successful synthesis of Pt_3Sn NPs was the coinjection of $Pt(acac)_2$ and $Sn(acac)_2$ at high temperatures. The size of the Pt_3Sn NPs was tuned from 4 to 7 nm by controlling the metal-injection temperatures. The Pt_3Sn alloy NPs were catalytically more active for CO and methanol oxidations than the pure Pt NP catalyst, and their activity and stability could be further improved by the thermal treatment in Ar + 5% H_2 at 400 °C for 1 h. The Pt_3Sn NPs are a promising group of new catalysts for electro-oxidation of CO, methanol, and other small organic molecules.

dx.doi.org/10.1021/cs200430r |*ACS Catal.* 2011, 1, 1719–1723

EXPERIMENTAL METHODS

Chemicals. $Pt(acac)_2$ (acac = acetylacetonate), $Sn(acac)_2$ (98%, Strem), oleylamine (OAm, technical grade, 70%, Aldrich), oleic acid (OA, technical grade, 90%, Aldrich), 1-octadecene (ODE, technical grade, 90%, Aldrich), benzyl ether (BE, 98%, Aldrich), carbon black (Kejen EC 300J), acetic acid (ACS reagent, ≥ 99.7%, Aldrich). E-TEK Pt (20% Pt loading, Fuel Cell Store), TANAKA Pt (TEC10E50E-HT, 50.5% Pt loading, TANAKA KIKINZOKU KOGYO K. K.), perchloric acid ($HClO_4$, 70−72%, J. T. Baker), methanol (≥99.8%, Mallinckrodt Chemicals) were purchased and used as received.

Synthesis of Pt_3Sn NPs. Under an argon (Ar) gas flow and magnetic stirring, 2 mL of OA and 15 mL of ODE were mixed in a reaction flask and degassed at room temperature and 120 °C for 0.5 h each. At the same time, a 5 mL BE solution of 0.15 mmol $Pt(acac)_2$ and 0.05 mmol $Sn(acac)_2$ was prepared separately by first dissolving 0.059 g of $Pt(acac)_2$ in 5 mL of BE with sonication, followed by addition of 0.11 mL of $Sn(acac)_2$ stock solution (0.5 mL $Sn(acac)_2$ in 4.5 mL of BE). The OA and ODE mixture was heated up to 220 °C when 3 mL of OAm was added by syringe. Once the reaction temperature reached 220 °C again, the BE solution of $Pt(acac)_2$ and $Sn(acac)_2$ was injected immediately to initiate the burst nucleation, which was indicated by the solution color change from light yellow to black for about 60 s after injection. Then the temperature was raised to 280 °C at a heating rate of 2 °C/min, and kept at this temperature for 1 h. After cooling down to room temperature, the Pt_3Sn NPs were separated by adding isopropanol and centrifugation. The Pt_3Sn NPs were washed twice by a mixture of hexane and isopropanol and finally dispersed in hexane. The size of as prepared Pt_3Sn was around 5.2 nm.

To prepare smaller (3.6 nm) and larger (6.6 nm) Pt_3Sn NPs, OAm and the metal precursor solution were injected at 180 and 240 °C respectively while other reaction conditions were kept same.

Preparation of Carbon Supported Pt_3Sn NPs (Pt_3Sn As Prepared). Ten milligrams of Pt_3Sn NPs in 15 mL of hexane were mixed with 30 mg of carbon black (Ketjen EC-300J) and sonicated for 1 h. The Pt_3Sn NPs loaded on carbon was separated by centrifugation and then heated in acetic acid at 70 °C for 12 h and washed with ethanol. After surfactant (25 wt % of the NPs, calculated from ICP data) removal, the total metal loading calculated was 20 wt %, and the Pt loading was 16% wt. Finally, the Pt_3Sn as prepared was dried under a controlled flow of nitrogen and dispersed in deionized (DI) water by sonication to form a 2 mg of catalyst per mL of suspension.

Thermal Annealing of the Carbon Supported Pt_3Sn As Prepared (Pt_3Sn Annealed). The Pt_3Sn NPs supported carbon black (Ketjen EC-300J) was annealed under a gentle flow of Ar + 5% H_2 in a tube furnace at 400 °C for 1 h. The annealed Pt_3Sn/C was dispersed in DI water to form a 2 mg of catalyst per mL of suspension.

Commercial Pt Catalysts. TANAKA Pt (50.5% Pt, 5 nm) was dispersed in DI water to form a 0.5 mg of catalyst/mL of suspension and used for CO oxidation. E-TEK Pt (20% Pt, 2−3 nm) was sonicated with DI water to form a 2 mg of catalyst/mL of suspension and used for methanol oxidation reaction (MOR).

Electrochemical Measurement. Twenty microliters of catalyst in water suspension (2 mg of catalyst/mL of water) was deposited on a glassy carbon rotating disk (5 mm in diameter, mirror polished) and dried under vacuum at room temperature. Ten microliters of 0.1 wt % Nafion water solution was deposited over the catalyst and dried. Ag/AgCl electrode and Pt wire were used as the reference and counter electrodes, respectively. All potentials used in the figures are versus Ag/AgCl.

In the CO experiments, the rotating disk electrode was first immersed in the CO saturated 0.1 M $HClO_4$ at −0.20 V to form a CO adlayer on the NP surface. The CO stripping voltammetry was performed by scanning between −0.20 and 0.70 V in the Ar purged 0.1 M $HClO_4$ at 50 mV/s sweep rate. The CO bulk oxidation polarization curves were acquired at 1600 rpm rotating speed and 20 mV/s sweep rate. The upper potential limit for the CO bulk oxidation was 0.30 V for the Pt_3Sn and 0.47 V for the Pt.

In the MOR experiments, the electrodes were first immersed in the nitrogen saturated 0.1 M $HClO_4$ solution, and the potential was scanned from −0.25 to 0.7 V at a scan rate of 50 mV/s. The scan was repeated several times to obtain a stable cyclic voltammogram (CV) curve. CVs were used to estimate the ECASA of the catalyst by calculating the H_{upd} area of the catalyst. CVs for MOR were conducted in 0.1 M $HClO_4$ and 0.1 M methanol from 0 to 0.7 V at a scan rate of 50 mV/s. The MOR currents were normalized to ECASAs or to Pt weight. The stability was tested by chronoamperometry at 0.3 V in 0.1 M $HClO_4$ and 0.1 M methanol for 1 h. The currents were also normalized with ECASAs or Pt weight. After the stability test, the electrode was rinsed with DI water then immersed in fresh 0.1 M $HClO_4$. Potential scan from −0.25 to 0.7 V at a scan rate of 50 mV/s was repeated to record a stable CV after the stability test.

Characterization. TEM and high resolution TEM (HRTEM) images were acquired on a Philips CM20 (200 kV) and a JEOL 2010 (200 kV) transmission electron microscope. X-ray powder diffraction patterns of the samples were recorded on a Bruker AXS D8-Advanced diffractometer with Cu K_α radiation (λ = 1.5418 Å). The compositions of the samples were measured by Inductively Coupled Plasma−Atomic Emission Spectroscopy (ICP-AES) and Energy Dispersive X-ray Spectroscopy (EDS) on a LEO 1560 scanning electron microscope. Electrochemical measurements were performed on a Pine Electrochemical Analyzer, Model AFCBP1.

ASSOCIATED CONTENT

Supporting Information. Additional TEM images, XRD patterns, elemental analysis data, and electrochemistry data of Pt_3Sn and Pt catalysts. This material is available free of charge via the Internet at http://pubs.acs.org.

AUTHOR INFORMATION

Corresponding Author

*Fax: (+1) 401-863-9046. E-mail: ssun@brown.edu.

Funding Sources

Supported in part by ExxonMobil Research and Engineering Co.

REFERENCES

(1) Chen, A.; Holt-Hindle, P. *Chem. Rev.* **2010**, *110*, 3767–3804.
(2) Ferrando, R.; Jellinek, J.; Johnston, R. L. *Chem. Rev.* **2008**, *108*, 845–910.
(3) Liu, Y.; Li, D.; Sun, S. *J. Mater. Chem.* **2011**, *21*, 12579–12587.
(4) Wang, D.; Li, Y. *Adv. Mater.* **2011**, *23* (9), 1044–1060.
(5) Kua, J.; Goddard, W. A. *J. Am. Chem. Soc.* **1999**, *121*, 10928–10941.

(6) Stamenkovic, V. R.; Mun, B. S.; Arenz, M.; Mayrhofer, K. J. J.; Lucas, C. A.; Wang, G.; Ross, P. N.; Markovic, N. M. *Nat. Mater.* **2007**, *6*, 241–247.
(7) Markovic, N. M.; Ross, P. N. *Surf. Sci. Rep.* **2002**, *45*, 117–229.
(8) Wang, Y.; Mi, Y.; Redmon, N.; Holiday, J. *J. Phys. Chem. C* **2010**, *114*, 317–326.
(9) Huidobro, A.; Sepulveda-Escribano, A.; Rodriguez-Reinoso, F. *J. Catal.* **2002**, *212*, 94–103.
(10) Santori, G. F.; Casella, M. L.; Siri, G. J.; Adúriz, H. R.; Ferrettia, O. A. *React. Kinet. Catal. Lett.* **2002**, *75*, 225–230.
(11) Merlo, A. B.; Vetere, V.; Ruggera, J. F.; Casella, M. L. *Catal. Commun.* **2009**, *13*, 1665–1669.
(12) Burch, R.; Garla, L. C. *J. Catal.* **1981**, *71*, 360–372.
(13) Llorca, J.; Homs, N.; Fierro, J. L. G.; Sales, J.; Piscina, P. R. d. l. *J. Catal.* **1997**, *166*, 44–52.
(14) Lieske, H.; Volter, J. *J. Catal.* **1984**, *90*, 96–105.
(15) Stamenkovic, V.; Arenz, M.; Blizanac, B. B.; Mayrhofer, K. J. J.; Ross, P. N.; Markovic, N. M. *Surf. Sci.* **2005**, *576*, 145–157.
(16) Stamenkovic, V. R.; Arenz, M.; Lucas, C. A.; Gallagher, M. E.; Ross, P. N.; Markovic, N. M. *J. Am. Chem. Soc.* **2003**, *125*, 2736–2745.
(17) Gasteiger, H. A.; Markovic, N. M.; Ross, P. N. *J. Phys. Chem.* **1995**, *99*, 8945–8949.
(18) Hayden, B. E.; Rendall, M. E.; South, O. *J. Am. Chem. Soc.* **2003**, *125*, 7738–7742.
(19) Gasteiger, H. A.; Marković, N. M.; Ross, P. N. *Catal. Lett.* **1996**, *36*, 1–8.
(20) Crabb, E. M.; Marshall, R.; Thompsett, D. *J. Electrochem. Soc.* **2000**, *147*, 4440–4447.
(21) Liu, Z.; Reed, D.; Kwon, G.; Shamsuzzoha, M.; Nikles, D. E. *J. Phys. Chem. C* **2007**, *111*, 14223–14229.
(22) Honma, I.; Toda, T. *J. Electrochem. Soc.* **2003**, *150*, A1689–A1692.
(23) Neto, A. O.; Dias, R. R.; Tusi, M. M.; Linardi, M.; Spinacé, E. V. *J. Power Sources* **2007**, *166*, 87–91.
(24) Vigier, F.; Coutanceau, C.; Hahn, F.; Belgsir, E. M.; Lamy, C. *J. Electroanal. Chem.* **2004**, *563*, 81–89.
(25) Melke, J.; Schoekel, A.; Dixon, D.; Cremers, C.; Ramaker, D. E.; Roth, C. *J. Phys. Chem. C* **2010**, *114*, 5914–5925.
(26) Jiang, L.; Zhou, Z.; Li, W.; Zhou, W.; Song, S.; Li, H.; Sun, G.; Xin, Q. *Energy Fuels* **2004**, *18*, 866–871.
(27) Neto, A. O.; Vasconcelos, T. R. R.; Silva, R. W. R. V. D.; Linardi, M.; Spinacé, E. V. *J. Appl. Electrochem.* **2005**, *35*, 193–198.
(28) Dupont, C.; Jugnet, Y.; Loffreda, D. *J. Am. Chem. Soc.* **2006**, *128*, 9129–9136.
(29) Boualleg, M.; Baudouin, D.; Basset, J.-M.; Bayard, F.; Candy, J.-P.; Jumas, J.-C.; Veyre, L.; Thieuleux, C. *Chem. Commun.* **2010**, *46*, 4722–4724.
(30) Beden, B.; Lamy, C.; de Tacconi, N. R.; Arvia, A. J. *Electrochim. Acta* **1990**, *35*, 691–704.
(31) Lee, S. W.; Chen, S.; Sheng, W.; Yabuuchi, N.; Kim, Y.-T.; Mitani, T.; Vescovo, E.; Shao-Horn, Y. *J. Am. Chem. Soc.* **2009**, *131*, 15669–15677.
(32) Sharma, S.; Ganguly, A.; Papakonstantinou, P.; Miao, X.; Li, M.; Hutchison, J. L.; Delichatsios, M.; Ukleja, S. *J. Phys. Chem. C* **2010**, *114*, 19459–19466.